Title

Enabling “Sodium—Metal-Free” Manufacturing of Solid-State Batteries

Authors

Tseng, Kang-Ting

Lee, Kiwoong

Sakamoto, Jeff

Publication Date

2024

DOI

10.1021/acsenergylett.4c01724

Peer reviewed

ACS Energy LETTERS

http://pubs.acs.org/journal/aelccp

Enabling "Sodium–Metal-Free" Manufacturing of Solid-State Batteries

Kang-Ting Tseng,[†] Kiwoong Lee,[†] and Jeff Sakamoto*

Cite This: *ACS Energy Lett.* 2024, 9, 4544–4549

Read Online

ACCESS | Metrics & More | Article Recommendations | Supporting Information

ABSTRACT: The Na–metal-free manufacturing approach can improve both the manufacturing and performance of Na metal solid-state batteries. While significant research has been dedicated to Li–metal-free manufacturing, the exploration of Na-based counterparts remains relatively nascent. Similar to Li–metal-free manufacturing, achieving uniform Na deposition remains a challenge when using a solid-state electrolyte. In this work, we demonstrated the ability to plate a uniform 2.0 mAh cm^{-2} Na metal anode by the simple placement of an Al foil-based current collector on NASICON solid-state electrolyte. The Na anode uniformity was dramatically improved by functionalizing the Al CC with a ∼96 nm thick layer of Au. It was shown that the *in situ* plated Na is homogeneous and dense and can be reversibly stripped and plated at a Coulombic efficiency of >90%. Our findings advance the understanding of Na nucleation and growth and offer insights into streamlining manufacturing processes for future all-solid-state Na anodes.

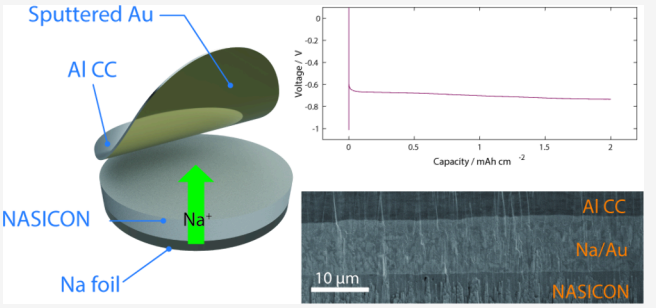

While lithium (Li)–metal solid-state batteries (LMSSBs) excel in higher energy density, sodium (Na)–metal solid-state batteries (SMSSBs) are increasingly viewed as the optimal choice for lighter duty vehicles and grid storage applications due to their advantages such as abundance in raw materials, sustainability, and cost-effectiveness.[1−4] Despite the apparent advantages over LMSSBs, similar to Li based system, Na metal is susceptible to reacting with oxygen and therefore complicates manufacturing.[5,6] To address this challenge, sodium–metal-free manufacturing (SMFM) can be suggested as an effective solution. SMFM can also provide a high purity Li/Na metal anode with a pristine interface after *in situ* deposition.[7−11] The SMFM process involves cell assembly in a discharged state and electrochemically transferring Na ions from the cathode to the solid electrolyte (SE)–current collector (CC) interface to electrodeposit metallic Na anodes *in situ*. This approach enhances energy density by eliminating excess Na and simplifies the manufacturing processes by removing the need to handle oxygen- and moisture-sensitive metallic Na. However, as it has been shown previously, it can be challenging to form a homogeneous metal anode.[7,12−14] Therefore, it is important to achieve the homogeneous nucleation of Na metal between the anode CC and the SE to avoid Na filament penetration due to current focusing.

Previous studies regarding LMSSBs made using SMFM employed methods such as the lamination of the anode CC, where the CC is diffusion bonded to SE at high temperature and pressure to ensure intimate contact between the CC and SEs,[7,15,16] or incorporating alloying anodes like an additional layer of Ag-C nanocomposite to achieve uniform and dendrite-free Li deposition.[17,18] Similarly, more recent studies regarding metal-free SMSSBs have explored using pelletized aluminum CCs[10] or thermal evaporation to deposit Cu layer onto NASICON as the CC[9] for improved SE–CC contact.

Building on the success of these approaches, it could be anticipated that similar principles would apply to SMSSBs. However, it is known that CC lamination onto SEs not only requires high temperature but also can introduce additional complications during plating due to overcoming adhesion between the SE and the CC.[15] Conversely, placing the CC directly on the SE can result in poor contact at the interface, leading to nonuniform plating and potential short-circuiting. Therefore, developing methods to enhance Na wetting on the CC, thereby facilitating uniform contact between anode CC and SE while promoting homogeneous Na plating, is crucial.

The use of alloying anodes has been extensively studied recently as they increase the lithiophilicity by introducing lithiophilic phases such as lithiated carbon materials and Li–

Received: June 26, 2024
Revised: August 15, 2024
Accepted: August 21, 2024

https://doi.org/10.1021/acsenergylett.4c01724
ACS Energy Lett. 2024, 9, 4544–4549

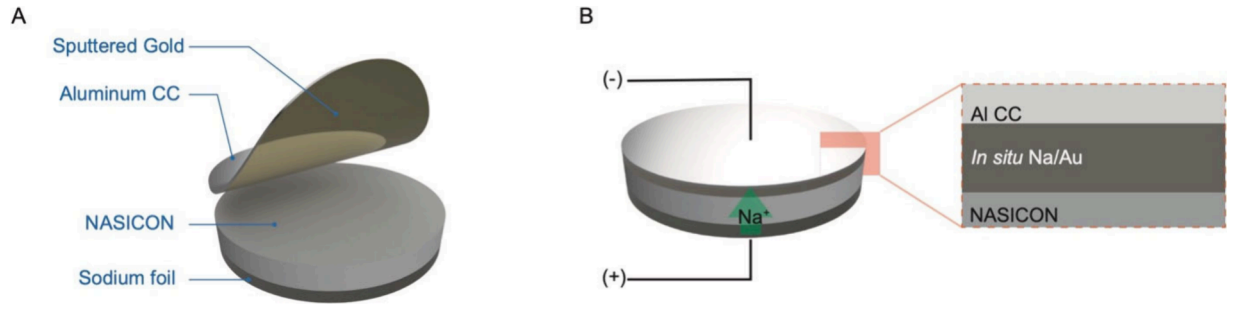

Figure 1. A schematic illustration of the cell configuration used in this study. (A) A custom-made Au−Al CC/NASICON/Na cell. (B) Depiction of the *in situ* plating of Na on the Au−Al CC.

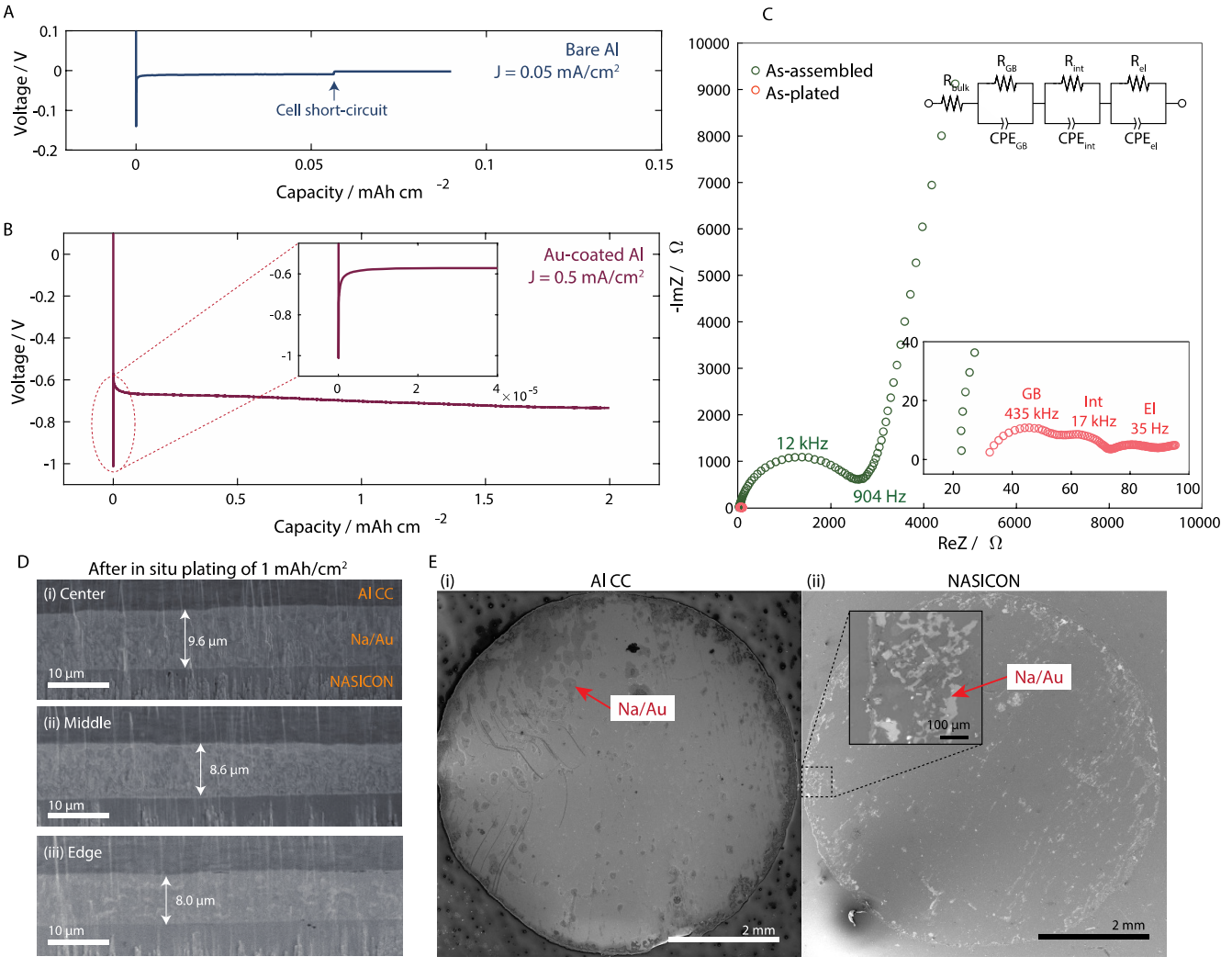

Figure 2. *In situ* plating of Na using a SMFM cell design. (A, B) Voltage profiles of *in situ* Na plating on (A) bare Al foil at 0.05 mA cm^{-2} and (B) Au−Al foil at 0.5 mA cm^{-2}. (C) Impedance spectra before (green circles) and after (red circles) *in situ* plating of Na on a Au−Al CC. (D) Cross-sectional images of *in situ* Na anodes at various electrode positions: (i) center, (ii) middle, and (iii) edge. (E) SEM images of Na nucleation immediately after Na deposition or 0.001 mAh cm^{-2}: (i) Au−Al CC and (ii) NASICON pellet.

metal (Li−M) alloys (M = Sn, Sb, Au, Ag).[17,19−22] Sandoval et al. showed that adding an additional layer of Ag or Au on the Cu CC improves Li nucleation density, enabling uniform Li growth across the CC.[13] Additionally, Haslam et al. demonstrated that sputtering Au onto LLZO to form Au−Li nanoclusters after heat treatment creates Li nucleation sites, facilitating homogeneous Li plating without the need for CC lamination.[12] Given the promise of alloying approaches, this study investigated whether similar strategies can be effective for Na-based systems as well.

We propose a simple method involving the attachment of a Au−aluminum (Al) CC on $Na_{3.4}Zr_2Si_{2.4}P_{0.6}O_{12}$ (NASICON) SE (Figure 1). In this study, NASICON was used as a model system owing to its low interfacial resistance against Na metal and the formation of kinetically stabled interphase.[23,24] This method demonstrates uniform nucleation/plating of metallic

https://doi.org/10.1021/acsenergylett.4c01724
ACS Energy Lett. 2024, 9, 4544−4549

Na between the anode CC and SE without Na filament penetration in the SE. After plating, subsequent stable cycling was achieved while maintaining the uniformity of the *in situ* formed Na (*in situ* Na) anode. Additionally, the use of Al foil as the CC in this study, as opposed to copper (Cu) foil, offers significant advantages for commercialization such as reducing the overall manufacturing costs[25] and increasing the energy density of the battery owing to its lighter weight than Cu. Thick Na foil was used as a counter electrode, as it serves as both a Na reservoir and a quasi-reference electrode.

As a control, bare Al foil was used as the CC. *In situ* plating of Na was attempted on this bare Al foil by using a current density of 0.05 mA cm^{-2} and a stack pressure of 5.6 MPa (Figure 2A). Different stack pressures were tested, and further details are available in the Supporting Information (Figure S2). A clear overpotential associated with Na nucleation was observed that was followed by a plateau, which was likely related to electrodeposition as has been observed previously.[9,26] The applied current was lower than the critical current density (CCD) measured for the NASICON pellet (1.9 mA cm^{-2}; see Figure S3). It should be noted that this CCD measurement is of a Na/NASICON/Na symmetric cell, establishing a much better electrode/SE contact compared to the cell that used bare Al CC. This could potentially lead to a localized current density much higher than the measured value.[27] Despite this consideration, cell short-circuiting occurred after the initiation of plating ($Q_{plate} \simeq 0.05$ mAh cm^{-2}; see Figure S4). This issue is attributed to inhomogeneous Na plating, resulting in localized current focusing. This likely caused subsequent Na filament initiation and penetration into the NASICON.[9]

Additionally, lamination of the Al CC onto the NASICON pellet with high temperature, following the method reported by Wang et al.,[15] was used to achieve homogeneous contact between the CC and the SE. However, cell short circuiting persisted (see Figure S5), showing that the lamination method, suitable for the LMSSB system, was inadequate for the SMSSB. Well-explored strategies for altering Li nucleation behavior involves incorporating a lithiophilic metal layer, such as Sn and Au.[12,28,29] These metals can form alloy clusters with Li on the surface, facilitating uniform Li deposition. Given the analogous working principles between Na and Li metal batteries, we hypothesized that incorporating a Au interlayer at the Al/NASICON interface could lower the energy barrier for Na deposition, leading to more homogeneous Na nucleation.

Cells were assembled by placing the Au−Al CC (Au thickness of ∼96 nm) on top of NASICON (Figure 1A) and conducted *in situ* plating of Na. The voltage profile for 2 mAh cm^{-2} of Na plating was achieved (Figure 2B), where the voltage response reached a minimum within the first few seconds, followed by a steady-state plateau (see Figure S6 for more details). This overpotential peak can be attributed to Na nucleation at the interface between Au−Al CC and NASICON. Moreover, it should be noted that the absence of a plateau above 0 V that indicates alloying behavior as seen by previous studies was observed. This is potentially due to kinetics limitations of Na−Au alloying compared to the alloying kinetics of Li−Au.[13] It is noteworthy that in the analogous study conducted by Haslam et al.[12] on the LLZO/Li system, the use of a flat Au layer led to short circuiting, contrasting with the findings in this study.

Figure 2C shows the electrochemical impedance spectra (EIS) of the cell before and after *in situ* Na plating in Figure 2B. Prior to *in situ* Na plating, a blocking tail in the low-frequency regime is evident, aligning with the semiblocking nature of the Au−Al CC. Additionally, a large bulk and grain boundary impedance was observed due to the poor contact between the CC and the NASICON. In contrast, the cell impedance after *in situ* plating exhibits a nonblocking behavior with three semicircles, representing impedance related to grain boundary and interface transport, and an electrochemical reaction, from high to low frequencies, respectively. The total interfacial resistance between NASICON and *in situ* Na was notably low, approximately 7 Ω cm^2, demonstrating the efficacy of using the Au coating in combination with the SMFM.

To verify the uniformity and conformality of *in situ* Na layer, cross sections of *in situ* Na/NASICON interfaces were prepared by focused ion beam (FIB) sectioning and observed by scanning electron microscopy (SEM). Parts i−iii of Figure 2D show the *in situ* Na/NASICON interface after Na plating of 1 mAh cm^{-2} (8.8 μm in thickness) at the different positions of the electrode, which are center, middle, and edge, respectively. This observation demonstrates that *in situ* plating of Na aided by the Au interlayer enabled a relatively uniform plating of Na without any additional methods. We hypothesize that in bare Al cell, Na plating was inhomogeneous, leading to current focusing, which in turn caused Na filament penetration and subsequent short-circuiting. In contrast, the Au layer facilitated the formation of a Na−Au alloy, thereby enhancing the wetting between the SE and the CC. This improved wetting promoted uniform Na deposition, effectively mitigating short-circuiting. These observations are consistent with the findings of Haslam et al., who demonstrated that an Au interlayer improved Li wetting, resulting in homogeneous Li deposition. In their study, the Au layer also prevented short-circuiting, whereas Li deposition without the Au interlayer led to inhomogeneous plating and eventual short-circuiting.

Additionally, energy dispersive spectroscopy (EDS) analysis (Figure S7) was conducted on an *in situ* formed Na layer in Figure 2D. The Au, initially coated on the Al CC, was observed to be uniformly dispersed in the Na layer through alloying with Na during the *in situ* plating process.

To further investigate the impact of the Au interlayer on the uniformity of Na plating, the initial nucleation of Na was investigated. Immediately after the nucleation occurred (based on the voltage curve), the Al CC was removed from the NASICON pellet and observed using SEM (Figure 2E). Dark blotches appeared and were confirmed to be identified as Na−Au alloys (Figure S8). The blotches were distributed uniformly across the interface between the Al CC and NASICON. It is important to note that the distribution of Na/Au alloy depends on the initial physical contact between the SE and CC. Due to the nature of the solid−solid interface, inhomogeneous physical contact and initial Na/Au alloy nuclei distribution were inevitable without additional treatment (Figure S9). However, the presence of a Au interlayer improves wetting at the interface between the SE and CC, resulting in uniform deposition of Na as shown in Figure 2D.

However, as shown in the EDS mapping of the *in situ* Na layer (Figure S7), Au alloyed with Na during the *in situ* plating and migrated throughout the Na anode thickness. In principle, after the cell is discharged with a Coulombic efficiency (CE) closer to 100%, the distribution and morphology of residual Au may differ from the as-assembled cell. This variation could impact the subsequent charge process especially considering

https://doi.org/10.1021/acsenergylett.4c01724
ACS Energy Lett. 2024, 9, 4544−4549

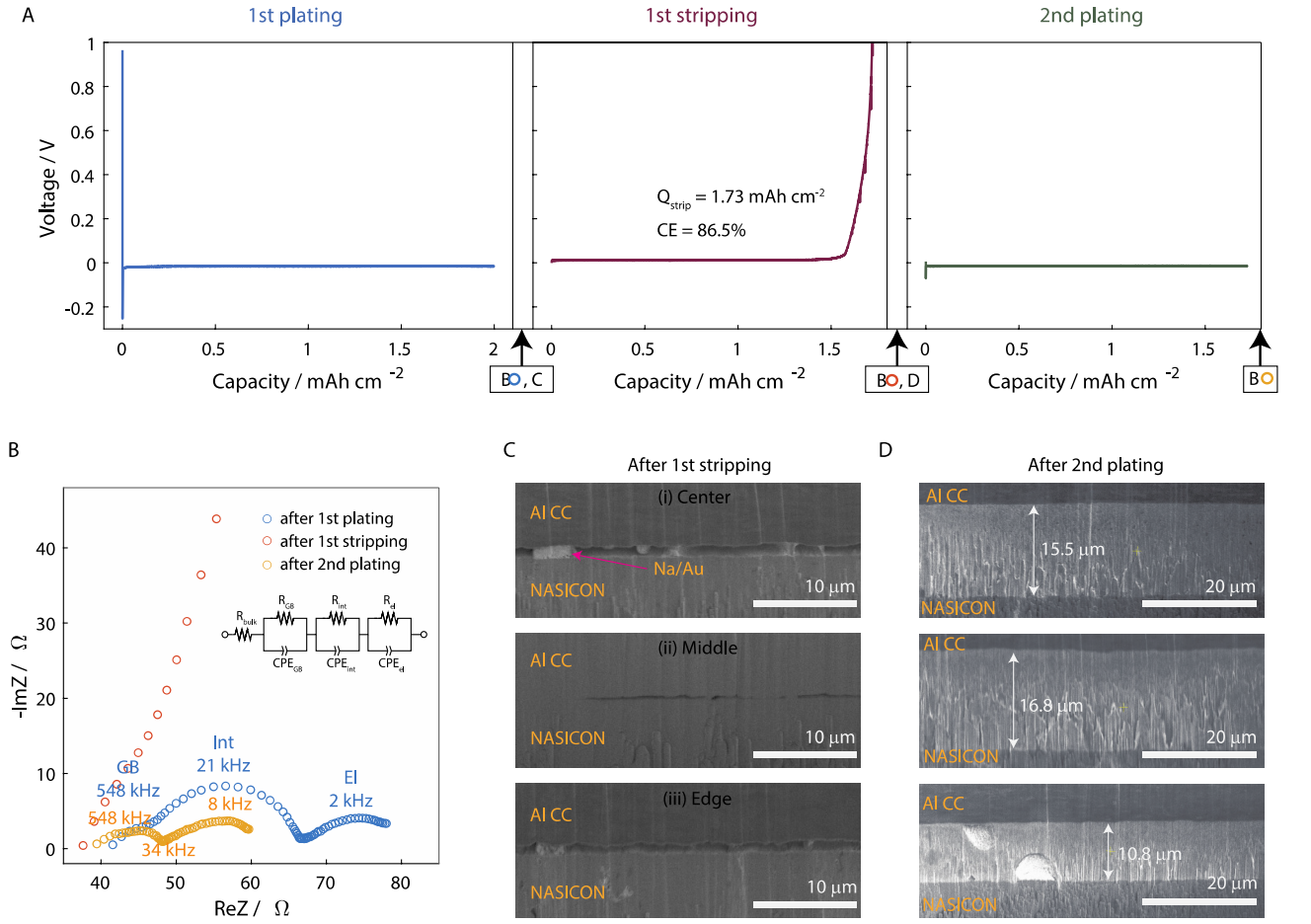

Figure 3. Behavior of subsequent *in situ* Na plating. (A) Potential profile during first cycle of plating and stripping of *in situ* Na plating at 0.5 mA cm^{-2} and 5.6 MPa. (B) Nyquist plot of the cell after the first and second *in situ* Na plating. (C) Cross-sectional SEM images of the cell after first stripping and (D) after second plating.

that the as-assembled cell features a uniformly coated Au layer. To address this concern, stripping and plating cycling were conducted, after *in situ* anode formation, to verify if the uniformity of Na was maintained.

Initially, 2.0 mAh cm^{-2} of Na was plated *in situ* between the Au−Al CC and NASICON at 0.5 mA cm^{-2} (blue line in Figure 3A) and then stripped again at the same current density until the voltage response approached the voltage cutoff of 1.5 V (illustrated by the red line in Figure 3A). Similar to the stripping of Li−metal anodes, the sudden increase in voltage during the stripping of *in situ* Na is attributed to the interfacial Na depletion, such as void formation and depletion observed with Li metal.[11,16,30,31] Cell impedance measured after the first stripping (Figure 3B) and *ex situ* FIB-SEM analysis (Figure 3C) following the first stripping demonstrated that the sudden increase in voltage response during stripping was attributed to Na depletion.[16] It is noteworthy that Na depletion occurred at relatively low CE, which was approximately 86.5% and 88.0% for the cells shown in Figure 3A and Figure 3C, respectively. This could possibly be attributed to the incomplete dealloying of Na from the Na−Au alloy. Additionally, the interface after stripping shows negligible remaining Na (Figure 3C). This suggests that some Na loss could be attributed to the irreversible solid electrochemical interphase (SEI) formation. Previous studies have indicated that there could be potential formation of SEI from the reduction of Zr[23,32] which could contribute to the low CE.

Subsequently, replating of Na was conducted to assess the Na uniformity. Several observations were made. First, there is a notable decrease in the nucleation overpotential between the first and second plating. Second, this phenomenon can be attributed to the remaining Na−Au alloy at the interface after stripping, contributing to enhanced wetting for Na deposition during the subsequent cycle. As mentioned earlier, due to the incomplete dealloying of Na during the preceding stripping, the Na−Au alloy could promote Na wetting, thus effectively lowering Na nucleation overpotential during the second plating as shown in Figures 3A and S10.[33,34] Additionally, this difference in thicknesses can be attributed to the likelihood of soft short-circuiting, as indicated as the spikey behavior during stripping cell polarization in Figure 3A.[31,35] To further investigate how the remaining Na/Au alloy at the interface after the first cycle affects the subsequent plating, Figure 3D presents a cross-sectional SEM analysis of the cell after the second plating. Notably, a marked difference in the thickness of the *in situ* plated Na, particularly at the edges, is observed. While theoretically, for a capacity of 2 mAh cm^{-2}, 17.6 μm of Na should be plated, the actual measurements show a discrepancy. Specifically, while the amount of Na plated at the center and middle closely aligns with the theoretical value (15.5 and 16.8 μm, respectively), the edge exhibits only 10.8 μm of *in situ* plated Na. Overall, the thickness is less than expected. This nonuniform plating can be attributed to the remaining Na and gaps formed at the Au−Al CC and

https://doi.org/10.1021/acsenergylett.4c01724
ACS Energy Lett. 2024, 9, 4544−4549

NASICON interface from the first cycle after stripping (as depicted in Figure 3C), which could lead to an inhomogeneous distribution of current density, resulting in preferential Na plating during subsequent plating.[36,37]

To demonstrate the viability of cycling SMSSB made using SMFM, proof of concept cells were cycled over 10 cycles at 0.2 mA cm^{-2} with a capacity of 2.0 mAh cm^{-2} at room temperature (Figure S11), where the CE was 94% after the tenth cycle. The cycling performance achieved in this study is similar to that of a comparable study conducted by Haslam et al.,[12] which is interesting to note since the homologous temperatures were the same in both studies (0.8). Despite both studies incorporating a Au interlayer to aid in Na or Li plating, they operate on fundamentally different principles. Haslam et al. observed that Au nanoclusters act as nucleation sites, facilitating stable Li plating. In contrast, our study demonstrates that the initially flat Au layer enhances wetting, promoting uniform Na deposition. Furthermore, our study shows evidence of unstable stripping behavior, contributing to a cycling performance that was not as optimal as that observed in the Li−Au study. Nevertheless, the behavior observed using a Au interlayer can serve as a guide for future work to focus on studying the stripping behavior and optimizing the stripping conditions as well as understanding the electrochemical−mechanical phenomena at the interface between Na and NASICON.

This study highlights the feasibility of the SMFM approach to make SMSSBs through the integration of the Au−Al CC. We have successfully demonstrated the stable *in situ* plating of Na at 0.5 mA cm^{-2} at room temperature, eliminating the necessity for high-temperature lamination to ensure intimate contact between the CC and the SE. In addition, it was revealed that upon stripping and replating, the Au−Na alloy remains consistently and uniformly distributed across the interface, indicating promising cyclability. This straightforward approach holds significant promise for advancing cost-effective and practical manufacturing processes in the development of SMFM for SMSSBs. However, given the high cost associated with Au metal, it is necessary to seek alternatives. Therefore, future work should explore cheaper substitutes for the metal interlayer.

■ ASSOCIATED CONTENT

Supporting Information

The Supporting Information is available free of charge at https://pubs.acs.org/doi/10.1021/acsenergylett.4c01724.

Detailed experimental methods, electrochemical performance at different stack pressures, CCD test, EDS mapping, and EIS fitting (PDF)

■ AUTHOR INFORMATION

Corresponding Author

Jeff Sakamoto − *Department of Materials Science and Engineering, University of Michigan, Ann Arbor, Michigan 48109, United States; Materials Department, University of California, Santa Barbara, Santa Barbara, California 93106, United States;* orcid.org/0000-0002-3099-462X; Email: sakamoto@ucsb.edu

Authors

Kang-Ting Tseng − *Department of Materials Science and Engineering, University of Michigan, Ann Arbor, Michigan 48109, United States*

Kiwoong Lee − *Department of Mechanical Engineering, University of Michigan, Ann Arbor, Michigan 48109, United States*

Complete contact information is available at: https://pubs.acs.org/10.1021/acsenergylett.4c01724

Author Contributions

†K.-T.T. and K.L. contributed equally to this work.

Notes

The authors declare the following competing financial interest(s): J.S. is the founder of Zakuro, Inc.

■ ACKNOWLEDGMENTS

K.L., K.-T.T., and J.S. acknowledge support from the Mechano-Chemical Understanding of Solid Ion Conductors, an Energy Frontier Research Center funded by the U.S. Department of Energy, Office of Science, Office of Basic Energy Science under Grant DE-SC0023438. The authors acknowledge the financial support of the University of Michigan College of Engineering and technical support from the Michigan Center for Materials Characterization. K.L. acknowledges support from the Kwanjeong Educational Foundation.

■ REFERENCES

(1) Zhao, L.; Zhang, T.; Li, W.; Li, T.; Zhang, L.; Zhang, X.; Wang, Z. Engineering of Sodium-Ion Batteries: Opportunities and Challenges. *Engineering* **2023**, *24*, 172−183.

(2) Ma, Q.; Tietz, F. Solid-State Electrolyte Materials for Sodium Batteries: Towards Practical Applications. *ChemElectroChem.* **2020**, *7* (13), 2693−2713.

(3) Janek, J.; Zeier, W. G. Challenges in Speeding up Solid-State Battery Development. *Nat. Energy* **2023**, *8* (3), 230−240.

(4) Sayahpour, B.; Li, W.; Bai, S.; Lu, B.; Han, B.; Chen, Y.-T.; Deysher, G.; Parab, S.; Ridley, P.; Raghavendran, G.; Nguyen, L. H. B.; Zhang, M.; Meng, Y. S. Quantitative Analysis of Sodium Metal Deposition and Interphase in Na Metal Batteries. *Energy Environ. Sci.* **2024**, *17* (3), 1216−1228.

(5) Lee, B.; Paek, E.; Mitlin, D.; Lee, S. W. Sodium Metal Anodes: Emerging Solutions to Dendrite Growth. *Chem. Rev.* **2019**, *119* (8), 5416−5460.

(6) Shi, H.; Zhang, Y.; Liu, Y.; Yuan, C. Metallic Sodium Anodes for Advanced Sodium Metal Batteries: Progress, Challenges and Perspective. *Chem. Rec.* **2022**, *22* (10), No. e202200112.

(7) Kazyak, E.; Wang, M. J.; Lee, K.; Yadavalli, S.; Sanchez, A. J.; Thouless, M. D.; Sakamoto, J.; Dasgupta, N. P. Understanding the Electro-Chemo-Mechanics of Li Plating in Anode-Free Solid-State Batteries with Operando 3D Microscopy. *Matter* **2022**, *5* (11), 3912−3934.

(8) Davis, A. L.; Kazyak, E.; Liao, D. W.; Wood, K. N.; Dasgupta, N. P. Operando Analysis of Interphase Dynamics in Anode-Free Solid-State Batteries with Sulfide Electrolytes. *J. Electrochem. Soc.* **2021**, *168* (7), No. 070557.

(9) Ortmann, T.; Fuchs, T.; Eckhardt, J. K.; Ding, Z.; Ma, Q.; Tietz, F.; Kübel, C.; Rohnke, M.; Janek, J. Deposition of Sodium Metal at the Copper-NaSICON Interface for Reservoir-Free Solid-State Sodium Batteries. *Adv. Energy Mater.* **2024**, *14*, No. 2302729.

(10) Deysher, G.; Oh, J. A. S.; Chen, Y.-T.; Sayahpour, B.; Ham, S.-Y.; Cheng, D.; Ridley, P.; Cronk, A.; Lin, S. W.-H.; Qian, K.; Nguyen, L. H. B.; Jang, J.; Meng, Y. S. An Anode-Free Sodium All-Solid-State Battery. *ChemRxiv* **2023**, DOI: 10.26434/chemrxiv-2023-tkcd9.

(11) Wang, M. J.; Choudhury, R.; Sakamoto, J. Characterizing the Li-Solid-Electrolyte Interface Dynamics as a Function of Stack Pressure and Current Density. *Joule* **2019**, *3* (9), 2165−2178.
(12) Haslam, C.; Sakamoto, J. Stable Lithium Plating in "Lithium Metal-Free" Solid-State Batteries Enabled by Seeded Lithium Nucleation. *J. Electrochem. Soc.* **2023**, *170* (4), No. 040524.
(13) Sandoval, S. E.; Lewis, J. A.; Vishnugopi, B. S.; Nelson, D. L.; Schneider, M. M.; Cortes, F. J. Q.; Matthews, C. M.; Watt, J.; Tian, M.; Shevchenko, P.; Mukherjee, P. P.; McDowell, M. T. Structural and Electrochemical Evolution of Alloy Interfacial Layers in Anode-Free Solid-State Batteries. *Joule* **2023**, *7* (9), 2054−2073.
(14) Liu, W.; Luo, Y.; Hu, Y.; Chen, Z.; Wang, Q.; Chen, Y.; Iqbal, N.; Mitlin, D. Interrelation Between External Pressure, SEI Structure, and Electrodeposit Morphology in an Anode-Free Lithium Metal Battery. *Adv. Energy Mater.* **2024**, *14* (5), No. 2302261.
(15) Wang, M. J.; Carmona, E.; Gupta, A.; Albertus, P.; Sakamoto, J. Enabling "Lithium-Free" Manufacturing of Pure Lithium Metal Solid-State Batteries through in Situ Plating. *Nat. Commun.* **2020**, *11* (1), 5201.
(16) Lee, K.; Kazyak, E.; Wang, M. J.; Dasgupta, N. P.; Sakamoto, J. Analyzing Void Formation and Rewetting of Thin in Situ-Formed Li Anodes on LLZO. *Joule* **2022**, *6* (11), 2547−2565.
(17) Lee, Y.-G.; Fujiki, S.; Jung, C.; Suzuki, N.; Yashiro, N.; Omoda, R.; Ko, D.-S.; Shiratsuchi, T.; Sugimoto, T.; Ryu, S.; Ku, J. H.; Watanabe, T.; Park, Y.; Aihara, Y.; Im, D.; Han, I. T. High-Energy Long-Cycling All-Solid-State Lithium Metal Batteries Enabled by Silver−Carbon Composite Anodes. *Nat. Energy* **2020**, *5* (4), 299−308.
(18) Tan, D. H. S.; Chen, Y.-T.; Yang, H.; Bao, W.; Sreenarayanan, B.; Doux, J.-M.; Li, W.; Lu, B.; Ham, S.-Y.; Sayahpour, B.; Scharf, J.; Wu, E. A.; Deysher, G.; Han, H. E.; Hah, H. J.; Jeong, H.; Lee, J. B.; Chen, Z.; Meng, Y. S. Carbon-Free High-Loading Silicon Anodes Enabled by Sulfide Solid Electrolytes. *Science* **2021**, *373* (6562), 1494−1499.
(19) Kwon, H.; Lee, J.-H.; Roh, Y.; Baek, J.; Shin, D. J.; Yoon, J. K.; Ha, H. J.; Kim, J. Y.; Kim, H.-T. An Electron-Deficient Carbon Current Collector for Anode-Free Li-Metal Batteries. *Nat. Commun.* **2021**, *12* (1), 5537.
(20) Chen, T.; Kong, W.; Zhao, P.; Lin, H.; Hu, Y.; Chen, R.; Yan, W.; Jin, Z. Dendrite-Free and Stable Lithium Metal Anodes Enabled by an Antimony-Based Lithiophilic Interphase. *Chem. Mater.* **2019**, *31* (18), 7565−7573.
(21) Zhang, S. S.; Fan, X.; Wang, C. A Tin-Plated Copper Substrate for Efficient Cycling of Lithium Metal in an Anode-Free Rechargeable Lithium Battery. *Electrochim. Acta* **2017**, *258*, 1201−1207.
(22) Shin, W.; Manthiram, A. Fast and Simple Ag/Cu Ion Exchange on Cu Foil for Anode-Free Lithium-Metal Batteries. *ACS Appl. Mater. Interfaces* **2022**, *14* (15), 17454−17460.
(23) Ortmann, T.; et al. Kinetics and Pore Formation of the Sodium Metal Anode on NASICON-Type Na3.4Zr2Si2.4P0.6O12 for Sodium Solid-State Batteries. *Adv. Energy Mater.* **2023**, *13*, 2202712.
(24) Oh, J. A. S.; Wang, Y.; Zeng, Q.; Sun, J.; Sun, Q.; Goh, M.; Chua, B.; Zeng, K.; Lu, L. Intrinsic Low Sodium/NASICON Interfacial Resistance Paving the Way for Room Temperature Sodium-Metal Battery. *J. Colloid Interface Sci.* **2021**, *601*, 418−426.
(25) Zhu, P.; Gastol, D.; Marshall, J.; Sommerville, R.; Goodship, V.; Kendrick, E. A Review of Current Collectors for Lithium-Ion Batteries. *J. Power Sources* **2021**, *485*, No. 229321.
(26) Cohn, A. P.; Muralidharan, N.; Carter, R.; Share, K.; Pint, C. L. Anode-Free Sodium Battery through in Situ Plating of Sodium Metal. *Nano Lett.* **2017**, *17* (2), 1296−1301.
(27) Fuchs, T.; Haslam, C. G.; Richter, F. H.; Sakamoto, J.; Janek, J. Evaluating the Use of Critical Current Density Tests of Symmetric Lithium Transference Cells with Solid Electrolytes. *Adv. Energy Mater.* **2023**, *13* (45), No. 2302383.
(28) Yan, K.; Lu, Z.; Lee, H.-W.; Xiong, F.; Hsu, P.-C.; Li, Y.; Zhao, J.; Chu, S.; Cui, Y. Selective Deposition and Stable Encapsulation of Lithium through Heterogeneous Seeded Growth. *Nat. Energy* **2016**, *1* (3), 1−8.
(29) Inaoka, T.; Asakura, T.; Otoyama, M.; Motohashi, K.; Sakuda, A.; Tatsumisago, M.; Hayashi, A. Tin Interlayer at the Li/Li3PS4 Interface for Improved Li Stripping/Plating Performance. *J. Phys. Chem. C* **2023**, *127* (22), 10453−10458.
(30) Kasemchainan, J.; Zekoll, S.; Jolly, D. S.; Ning, Z.; Hartley, G. O.; Marrow, J.; Bruce, P. G. Critical Stripping Current Leads to Dendrite Formation on Plating in Lithium Anode Solid Electrolyte Cells. *Nat. Mater.* **2019**, *18* (10), 1105−1111.
(31) Krauskopf, T.; Hartmann, H.; Zeier, W. G.; Janek, J. Toward a Fundamental Understanding of the Lithium Metal Anode in Solid-State Batteries—An Electrochemo-Mechanical Study on the Garnet-Type Solid Electrolyte $Li_{6.25}Al_{0.25}La_3Zr_2O_{12}$. *ACS Appl. Mater. Interfaces* **2019**, *11* (15), 14463−14477.
(32) Wang, C.; Sun, Z.; Zhao, Y.; Wang, B.; Shao, C.; Sun, C.; Zhao, Y.; Li, J.; Jin, H.; Qu, L. Grain Boundary Design of Solid Electrolyte Actualizing Stable All-Solid-State Sodium Batteries. *Small* **2021**, *17* (40), No. 2103819.
(33) Tang, S.; Qiu, Z.; Wang, X.-Y.; Gu, Y.; Zhang, X.-G.; Wang, W.-W.; Yan, J.-W.; Zheng, M.-S.; Dong, Q.-F.; Mao, B.-W. A Room-Temperature Sodium Metal Anode Enabled by a Sodiophilic Layer. *Nano Energy* **2018**, *48*, 101−106.
(34) Tang, S.; Zhang, Y.-Y.; Zhang, X.-G.; Li, J.-T.; Wang, X.-Y.; Yan, J.-W.; Wu, D.-Y.; Zheng, M.-S.; Dong, Q.-F.; Mao, B.-W. Stable Na Plating and Stripping Electrochemistry Promoted by In Situ Construction of an Alloy-Based Sodiophilic Interphase. *Adv. Mater.* **2019**, *31* (16), No. 1807495.
(35) Sastre, J.; Futscher, M. H.; Pompizi, L.; Aribia, A.; Priebe, A.; Overbeck, J.; Stiefel, M.; Tiwari, A. N.; Romanyuk, Y. E. Blocking Lithium Dendrite Growth in Solid-State Batteries with an Ultrathin Amorphous Li-La-Zr-O Solid Electrolyte. *Commun. Mater.* **2021**, *2* (1), 1−10.
(36) Lewis, J. A.; Sandoval, S. E.; Liu, Y.; Nelson, D. L.; Yoon, S. G.; Wang, R.; Zhao, Y.; Tian, M.; Shevchenko, P.; Martínez-Pañeda, E.; McDowell, M. T. Accelerated Short Circuiting in Anode-Free Solid-State Batteries Driven by Local Lithium Depletion. *Adv. Energy Mater.* **2023**, *13* (12), No. 2204186.
(37) Lee, K.; Sakamoto, J. Effect of Depth of Discharge (DOD) on Cycling in Situ Formed Li Anodes. *Faraday Discuss.* **2024**, *248* (0), 250−265.

https://doi.org/10.1021/acsenergylett.4c01724
ACS Energy Lett. 2024, 9, 4544−4549